Oxygen permeability of silicon-containing network polyamide and copolyamide films

Tsuyoshi Kiyotsukuri, Masaharu Mimaki and Naoto Tsutsumi
Department of Polymer Science and Engineering, Kyoto Institute of Technology, Matsugasaki, Sakyo-ku, Kyoto 606, Japan
(Received 9 July 1990; revised 30 July 1990; accepted 2 August 1990)

Network polyamide films (EY) of trimesic acid (Y) and 1,3-bis(3-aminopropyl)tetramethyldisiloxane (E), and network copolyamide films (EY/E*n*) of Y and E with aliphatic dicarboxylic acids (*n*) and those (EY/EE′) of Y and E with 1,3-bis(3-carboxypropyl)tetramethyldisiloxane (E′) were prepared. The prepolymer was prepared using a melt polycondensation method, and then a dimethylformamide solution of the prepolymer was cast on an aluminium plate. The cast film obtained was post-polymerized to form a network structure. Post-polymerized films were flexible, transparent and insoluble in common solvents. The molecular and supramolecular structures of these network polymers were characterized by infra-red absorption spectra, X-ray diffraction analysis, differential thermal analysis and thermomechanical analysis. Oxygen and nitrogen permeabilities increased with increasing temperature. EY homopolymer had P_{O_2} of 4.6×10^{-10} cm^3(s.t.p.) cm cm^{-2} s^{-1} cmHg^{-1} and P_{O_2}/P_{N_2} of 3.4 at 60°C. Incorporation of copolymer components E*n* and EE′ enhanced the oxygen and nitrogen permeabilities while decreasing the glass transition temperature (T_g). The decrease of T_g increased P_{O_2}, which may be explained by enhancement of the flexibility of the molecular chain. For the EY/EE′ copolymer, an increase in the EE′ component gave rise to an increase of P_{O_2} and a smaller decrease of P_{O_2}/P_{N_2}. The EY/EE′(10/90 mol%) film had the highest value of P_{O_2} of 3.2×10^{-9} cm^3(s.t.p.) cm cm^{-2} s^{-1} cmHg^{-1} and P_{O_2}/P_{N_2} of 2.8 at 60°C.

(Keywords: oxygen permeability; silicon-containing network film; siloxane moiety; glass transition temperature; flexibility of molecular chain; polyamides)

INTRODUCTION

Silicon-containing polyamides[1–7] have been investigated for the purpose of improving processability, thermo-oxidative stability and mechanical properties. The oxygen permeability of silicon-containing polymers has been extensively investigated for the application of these materials to fuel combustion systems and in purification of air for medical purposes[8]. We have synthesized polyamides[9], copolyamides[10] and polyimides[11] with siloxane moieties in their main chains, and polyamides and polyesters with siloxane moieties in their side-chains[12], and have characterized their properties and oxygen permeability. Furthermore, we have synthesized novel network polyesters[13–15] and polyamides[16], and have investigated their high resistance to heat distortion. Recently, we synthesized novel network polyamides and copolyamides with siloxane moieties in their main chains.

In this study, we report on a method of preparation of these novel network polyamides and copolyamides with siloxane moieties in their main chains, and discuss the molecular structure, thermal properties as well as oxygen permeability of these network polymers.

EXPERIMENTAL

Monomers

Figure 1 shows the structural formulae and codes of the tricarboxylic and dicarboxylic acids and diamine monomers. Trimesic acid triethyl ester was obtained by refluxing trimesic acid (Y) in ethanol at 80°C for 4 h in the presence of H_2SO_4 as a catalyst. The trimesic acid triethyl ester obtained was recrystallized from ethanol solution and then dried at 50°C for 24 h *in vacuo*. 1,3-Bis(3-aminopropyl)tetramethyldisiloxane (E) and 1,3-bis(3-carboxypropyl)tetramethyldisiloxane (E′), donated by Chisso Corp., Japan, were used without further purification. Malonic acid diethyl ester (3), adipic acid (6), azelaic acid (9) and 1,10-decanedicarboxylic acid (12) were used as received.

Preparation of prepolymers

A mixture of trimesic acid triethyl ester and E, in which aliphatic dicarboxylic acid was added for copolymerization, was heated up from room temperature to 140°C for 1–1.5 h, and further heated to 190–220°C at the rate of 0.5°C min^{-1}.

Film preparation

The obtained prepolymer was cast on an aluminium plate from 12 wt% dimethylformamide (DMF) solution at 80–100°C.

Post-polymerization of films

The cast film was post-polymerized under a stream of nitrogen in an electric furnace. After the aluminium substrate was dissolved off in a 10 wt% sodium hydroxide solution, a transparent and flexible film was obtained.

Characterization

The molecular-weight distribution of the prepolymer was determined by a Toyo Soda HLC-802A gel permeation chromatograph with TSK gel G2000H column standardized by polystyrene.

Thermomechanical analysis (t.m.a.) was performed in

0032-3861/91/142605-07

Diamine monomer

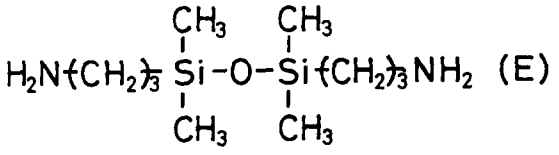

Triacid monomer

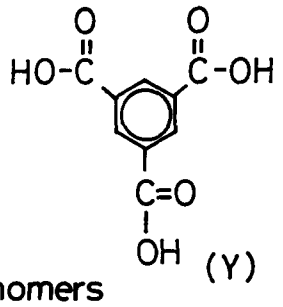

Diacid monomers

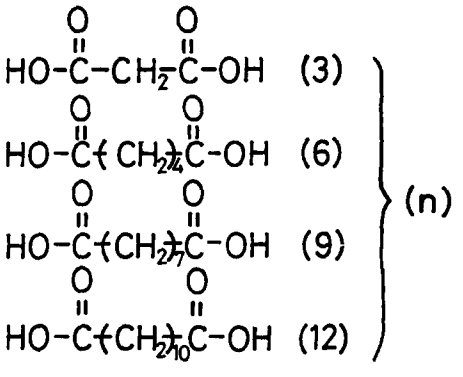

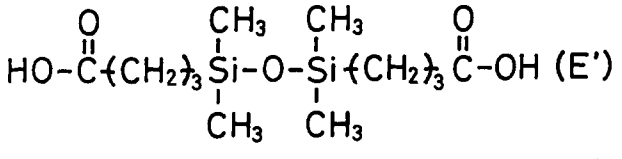

Figure 1 Structural formulae and codes of chemicals used in this study

the penetration mode under 10 kg cm^{-2} pressure at a heating rate of 10°C min^{-1} in nitrogen atmosphere, using a Shimadzu model DT-30 thermomechanical analyser.

Infra-red spectra were recorded on a Jasco model IR A-1 spectrophotometer using a KBr pellet or a thin film.

X-ray diffraction intensity was measured with a Toshiba model ADG-301 X-ray diffractometer with nickel-filtered Cu Kα radiation.

Differential thermal analysis (d.t.a.) was carried out on a Shimadzu model DT-30 differential thermal analyser at a heating rate of 10°C min^{-1} in nitrogen atmosphere.

Thermogravimetry (t.g.) was performed on a Shimadzu model DT-30 thermogravimetric analyser at a heating rate of 10°C min^{-1} in nitrogen atmosphere.

Gas permeability

Gas permeability was measured by Rikaseiki model K-315-N equipped with an MKS Baratron pressure transducer. The volume of gas permeating through a polymer film from upstream (including the permeation gas) to downstream in a vacuum of 0.1 mmHg was measured by the pressure transducer. The permeability coefficient P was calculated by the equation:

$$P = \frac{dp}{dt}\frac{L}{A}\frac{T_0}{p_0}\frac{1}{p}\frac{V}{T}$$

where dp/dt is the slope at steady state in the permeation curves, L is film thickness, A is film area, T_0 and p_0 are the temperature and pressure under standard conditions, p is the pressure of supplied gas, V is the cell volume downstream (including the pressure transducer) and T is the temperature of cell.

RESULTS AND DISCUSSION

Homopolymer film

Conditions of synthesis. Figure 2 shows the g.p.c. curve of EY prepolymer prepared by heating to 220°C at a rate of 0.5°C min^{-1}. *Table 1* illustrates the molecular structures

Table 1 Molecular structures of EY prepolymers estimated from the observed molecular weight; numbers 1–5 correspond to those in *Figure 2*

No.	Structure[a]	Molecular weight	
		Calc.	Obs.
1		248	150
2	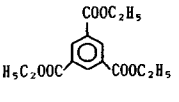	294	312
3	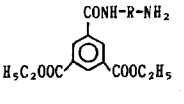	496	459
4	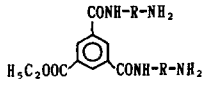	698	672
5	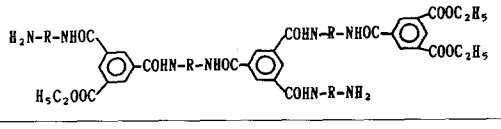	1526	1532

[a] R = 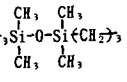

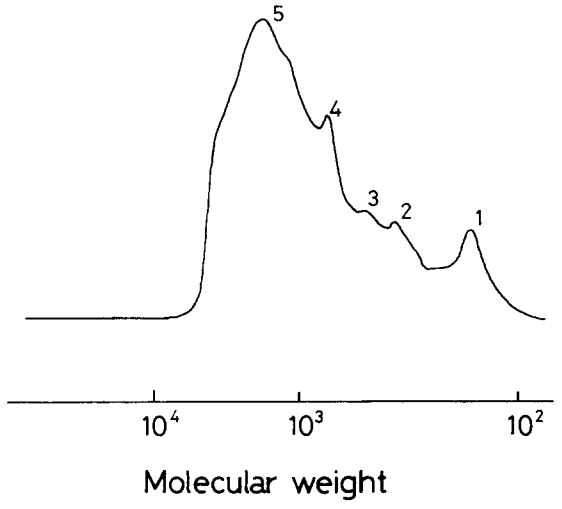

Figure 2 G.p.c. curve of EY prepolymer

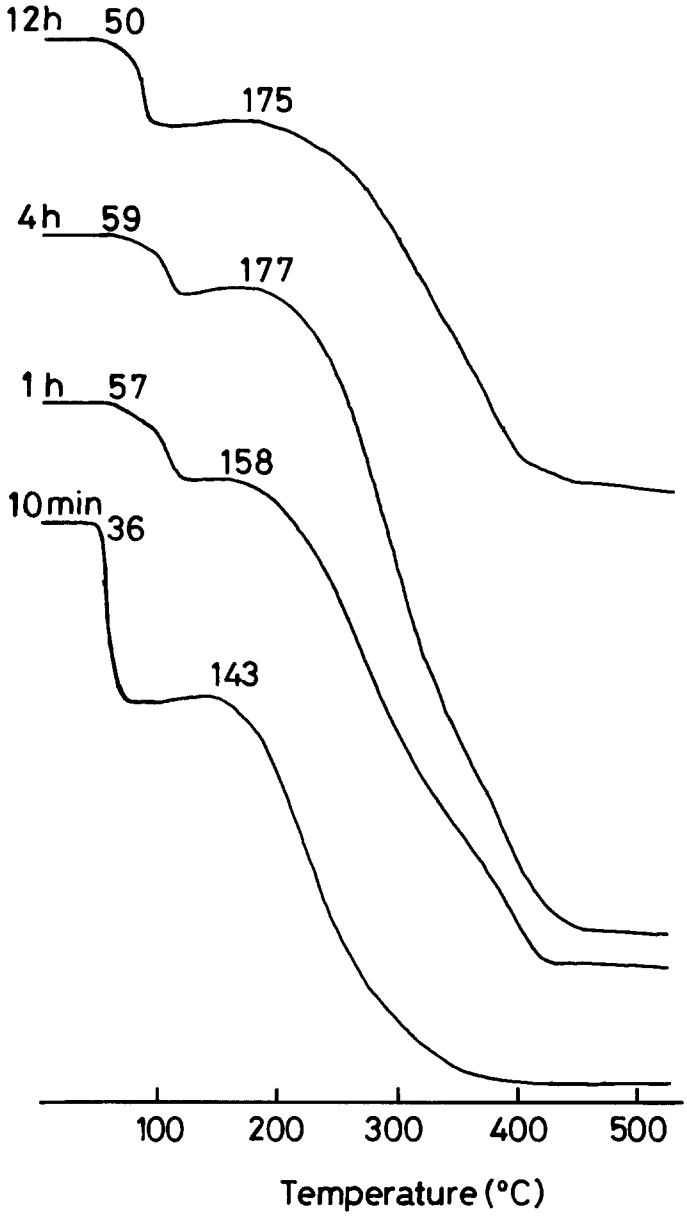

Figure 3 T.m.a. curves of EY post-polymerized for various times at 280°C

of prepolymer estimated from the observed molecular weights of peaks 1–5 in *Figure 2*. The estimated molecular structure in *Table 1* shows that the polymerization progresses stepwise and the molecular chain extends to two or three dimensions.

After casting the obtained prepolymer, it was post-polymerized to form a network. *Figure 3* shows the t.m.a. curves of EY post-polymerized for various times at 280°C, in which the t.m.a. probe penetrates into the polymer film stepwise. The inflection point of the t.m.a. curve, the heat distortion temperature, increases with increasing post-polymerization time. The dependence of the distortion temperature on the post-polymerization time at temperatures of 240, 280 and 300°C is shown in *Figure 4*. The first and second distortion temperatures increase with increasing post-polymerization time and level out above a post-polymerization time of 4 h. A film post-polymerized at higher temperature has a higher second distortion temperature, but there is no significant difference between the first distortion temperatures among three films post-polymerized at various temperatures. The second distortion temperature of EY corresponds to the heat distortion temperature of 187°C for 9Y having the same number of bonds per repeat unit in the main chain[16]. A film post-polymerized at 300°C considerably coloured, probably because of partial thermal decomposition at high temperature. Therefore the post-polymerization temperature and time were set as 280°C and 4 h. All post-polymerized films were flexible and transparent and insoluble in common solvents.

Structure and properties. Infra-red absorptions due to Si–O stretching, C=O stretching (amide I) and

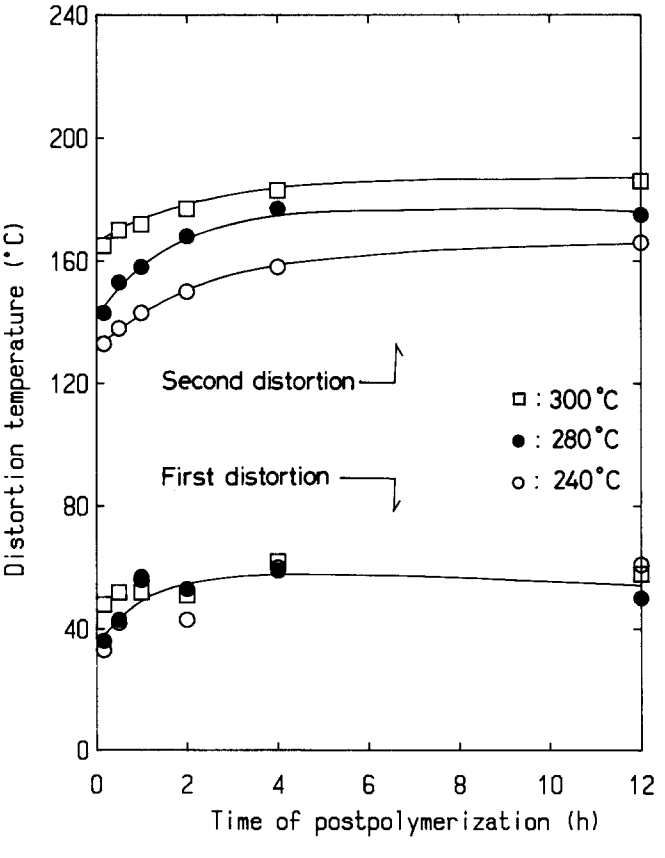

Figure 4 Plots of first and second distortion temperatures of EY against post-polymerization time

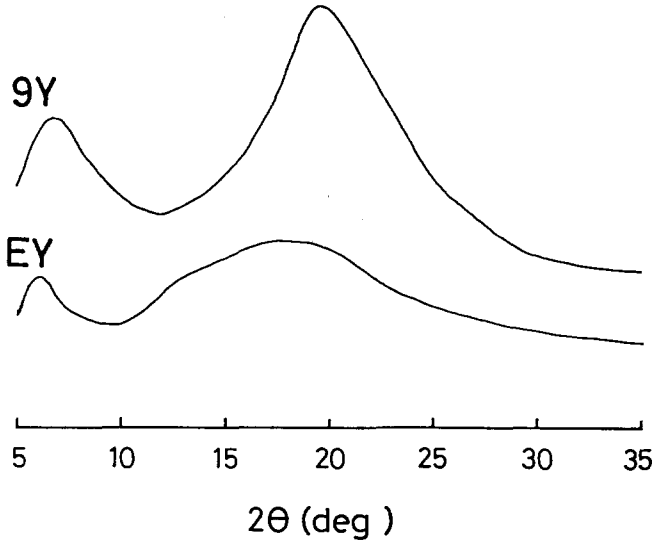

Figure 5 X-ray diffraction intensity curves of EY and 9Y

N–H bending (amide II) were confirmed at 1050, 1640 and 1540 cm^{-1}, respectively. The absorption peak at 1720 cm^{-1} due to C=O stretching of free carboxylic acid decreased with increasing post-polymerization time. The ratio between the absorbance at 1720 cm^{-1} and that at 1640 cm^{-1} decreased with post-polymerization time and almost levelled off above a post-polymerization time of 4 h, which corresponds well to the fact that the distortion temperature is almost levelled out above a post-polymerization time of 4 h as shown in *Figure 4*.

Figure 5 shows a comparison of X-ray diffraction curves of EY and 9Y. Both EY and 9Y have two broad but distinct peaks. The spacings for EY calculated using Bragg's equation are 14.7 and 4.9 Å, corresponding to the peaks of $2\theta = 6°$ and 18°, respectively. The diffraction around 6° may be ascribed to that from some ordered structure due to the alignment of the benzene ring in the direction of the main chain; and that around 18° is probably related to the intermolecular alignment of the benzene ring. The diffraction peak around 18° of EY is broader than that of 9Y, which implies that steric hindrance of the dimethyl side-group in component E may depress the formation of an ordered structure. D.t.a. showed two endothermic transitions at 46 and 104°C for EY. The lower transition temperature corresponds to the first distortion temperature measured by t.m.a. At the present stage, we do not have an exact answer for the appearance of two endothermic transitions, but we consider that the lower endothermic transition is the glass transition temperature. T.g. gave the temperature of 10% weight loss as 414 and 410°C and the residue at 600°C of 18 and 16% for EY and 9Y, respectively, showing that the thermal stability of component E is comparable to that of the methylene chain.

Gas permeability. Figure 6 shows the temperature dependence of permeability coefficients of oxygen (P_{O_2}) and nitrogen (P_{N_2}). The notation T_i in this figure will be discussed later. The activation of the segmental motion with increasing temperature makes the free volume larger, and thus the permeation of oxygen and nitrogen is enhanced by increasing temperature. The values P_{O_2} of 4.6×10^{-10} cm^3(s.t.p.) cm cm^{-2} s^{-1} $cmHg^{-1}$ and P_{O_2}/P_{N_2} of 3.4 were obtained at 60°C. We have reported that silicon-containing polyamide of E6 prepared from E and adipic acid has P_{O_2} of 20.4×10^{-10} cm^3(s.t.p.) cm cm^{-2} s^{-1} $cmHg^{-1}$ and P_{O_2}/P_{N_2} of 2.7 at 60°C[9]. The Si content of E6 of 15.6 wt% is comparable to that of EY of 15.9%. Thus, the lower P_{O_2} value of EY is probably ascribed to the rigid Y molecule. Therefore, we tried to obtain more oxygen-permeable film through the incorporation of a flexible aliphatic chain by copolymerization, as studied below.

Copolymer films

Structure and properties. Figure 7 shows the X-ray diffraction curves of EY/E*n* and EY/EE′ with EY content of 50 mol% as well as EY homopolymer. The intensity around 6° decreases with the incorporation of aliphatic copolymer component owing to a decrease in the network.

D.t.a. curves are shown in *Figures 8a* for EY/E*n* and *8b* for EY/EE′. The observed endothermic transition corresponds to the glass transition of these copolymers. The glass transition temperature (T_g) decreases on increasing the length of methylene chains in the aliphatic copolymer component, which is ascribed to the flexibility of aliphatic molecular chains. The increase of EE′ component in EY/EE′ also decreases T_g.

Table 2 shows the temperature of 10% weight loss and the residue at 600°C measured by t.g. Increase in the length of methylene chains in the aliphatic copolymer component leads to a decrease in the temperature of 10% weight loss, while the residue at 600°C is almost the same for all copolymers irrespective of the kind of aliphatic copolymer component.

Gas permeability. Figure 9 shows the temperature dependence of P_{O_2} and P_{N_2} for EY/E9(50/50 mol%) copolymer. No significant hysteresis of the permeability is observed during heating and cooling through the glass transition temperature. The slope of the Arrhenius plot

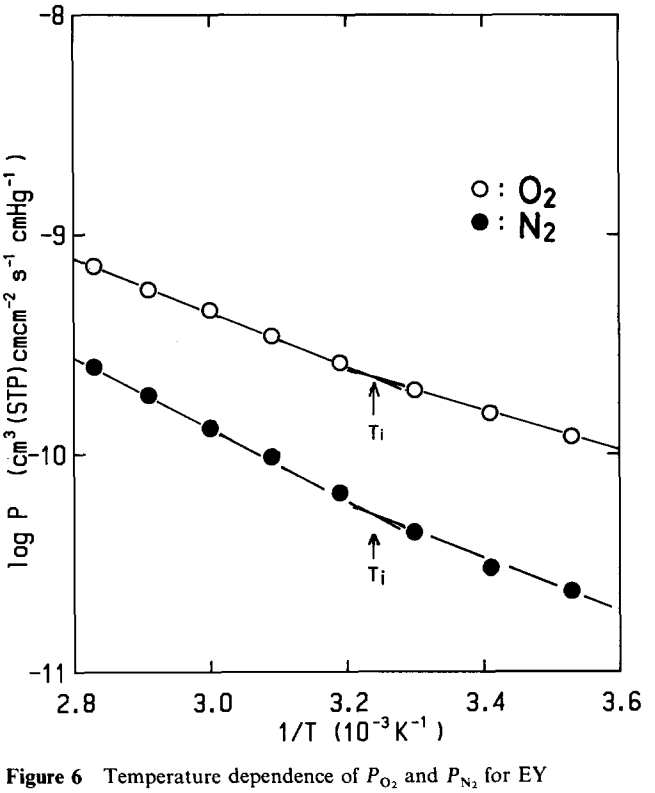

Figure 6 Temperature dependence of P_{O_2} and P_{N_2} for EY

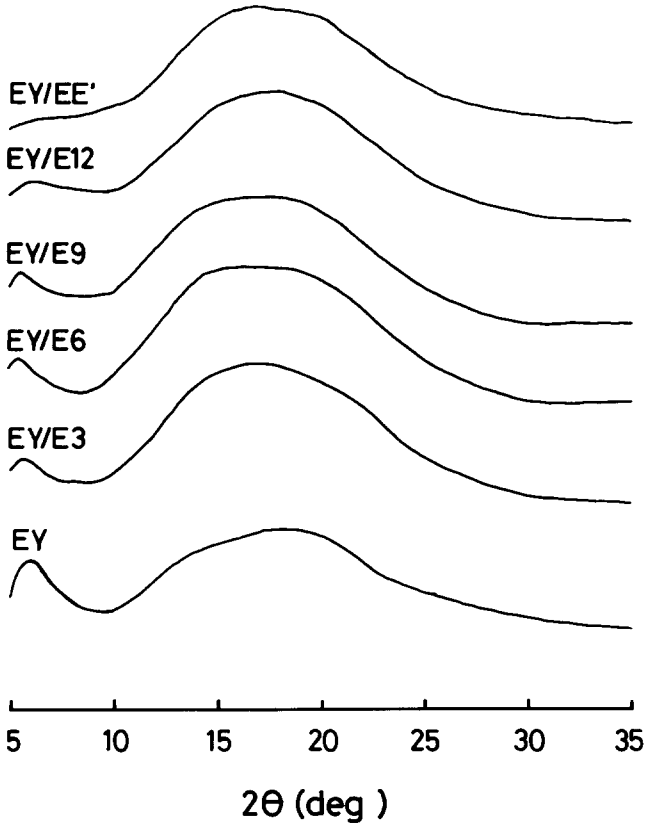

Figure 7 X-ray diffraction intensity curves of EY/E*n*

of the permeability coefficient is different above and below T_i. Other polymer films of EY/E3, EY/E6, EY/E12, EY/EE′ and EY also showed similar behaviour on the temperature dependence of the permeability coefficient. The T_i value is plotted against the glass transition temperature (T_g) of each polymer in *Figure 10*. A linear relationship between T_i and T_g is obtained, although T_g is $\sim 10°C$ higher than T_i: T_i is regarded as a transition temperature for gas permeability; T_g is the temperature at which micro-Brownian motion commences, and segmental mobility is largely enhanced above T_g, and thus the dependence of permeability on temperature might be changed.

Figure 11 shows the dependence on Si content of P_{O_2} of EY/E*n* and EY/EE′ as well as EY. P_{O_2} increases with decreasing Si content. This result suggests that silicon content is not the only factor affecting the higher permeation of oxygen in silicon-containing polymers. These permeabilities are replotted against the T_g of each polymer in *Figure 12*. P_{O_2} increases with decreasing T_g, which shows that the segmental mobility estimated by T_g dominates the permeation of oxygen. The longer methylene chains in the copolymer unit reduce T_g and therefore enhance P_{O_2}. In *Figure 12*, it is noted that EY/EE′ has larger P_{O_2} in spite of higher T_g. *Figure 13* shows the Si content dependence of P_{O_2} on changing the EE′ content in EY/EE′. In this case, P_{O_2} increases with increasing Si content and with decreasing T_g. EY/EE′(10/90 mol%) had the highest value of P_{O_2} of 3.2×10^{-9} cm^3(s.t.p.) cm cm^{-2} s^{-1} cmHg^{-1} and P_{O_2}/P_{N_2} of 2.8 at 60°C.

The values of P_{O_2} are plotted against the separation factor for all samples in *Figure 14*. Increase of P_{O_2} gives a decrease of P_{O_2}/P_{N_2}. It is noted that the relation between P_{O_2} and P_{O_2}/P_{N_2} for EY/EE′ is different from

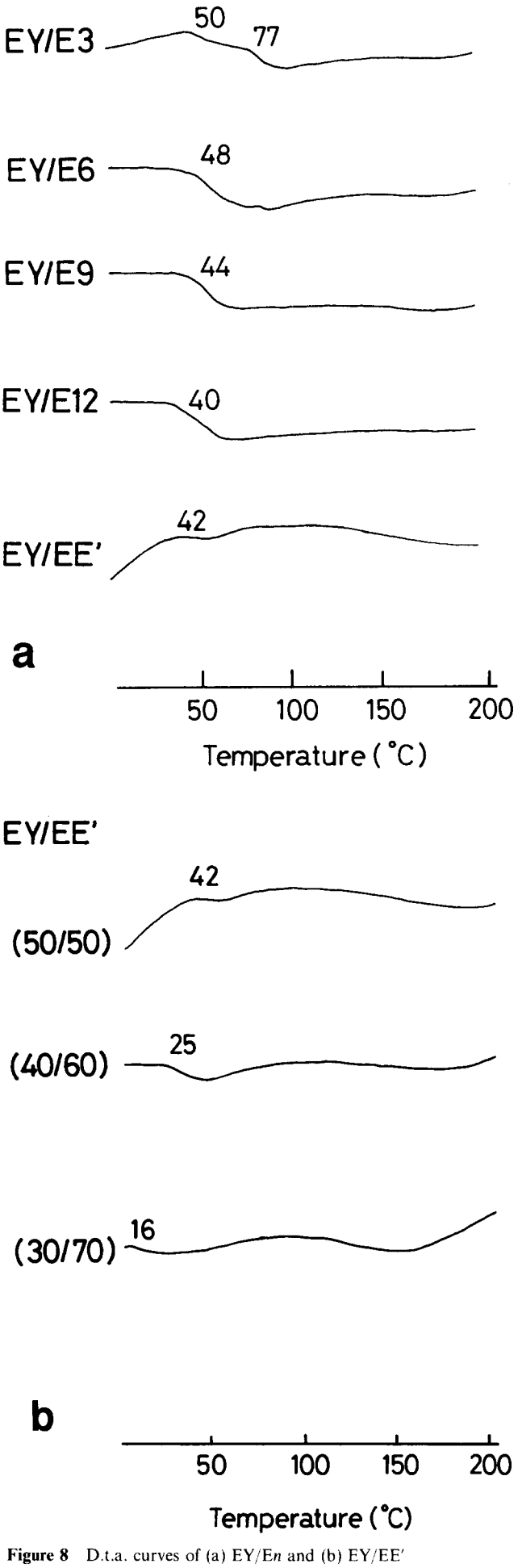

Figure 8 D.t.a. curves of (a) EY/E*n* and (b) EY/EE′

Table 2 Temperature of 10% weight loss and residue at 600°C for EY/E*n*(50/50 mol%) and EY/EE′(50/50 mol%)

Polymer	Temp. of 10% weight loss (°C)	Residue at 600°C (%)
EY/E3	430	16
EY/E6	399	16
EY/E9	389	16
EY/E12	379	15
EY/EE′	372	15

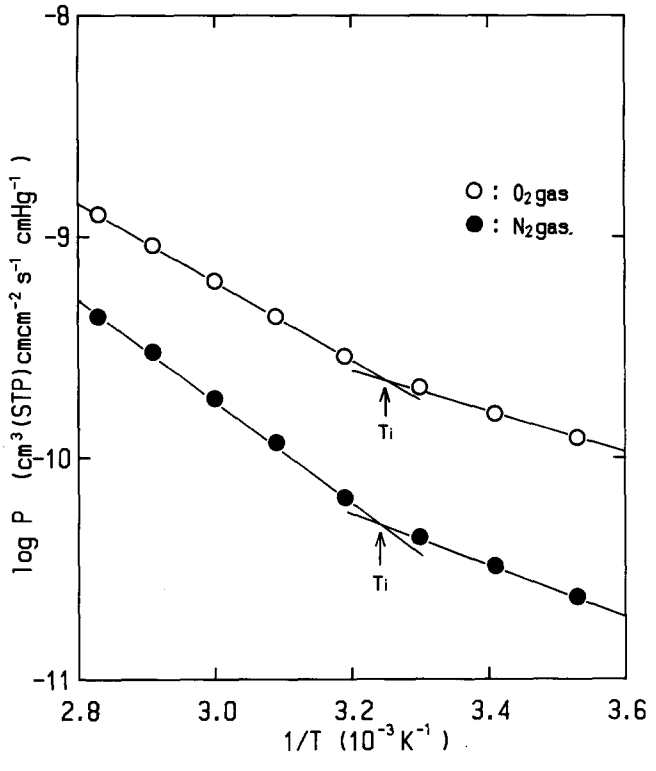

Figure 9 Temperature dependence of oxygen and nitrogen permeabilities for EY/E9(50/50 mol%)

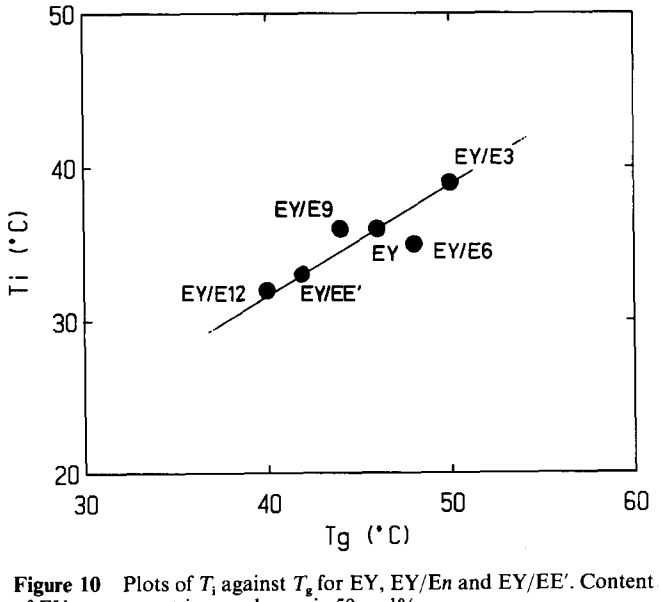

Figure 10 Plots of T_i against T_g for EY, EY/E*n* and EY/EE′. Content of EY component in copolymer is 50 mol%

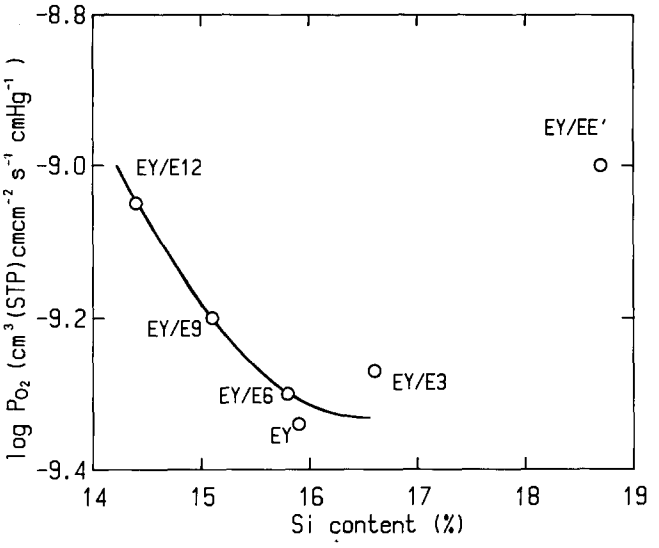

Figure 11 Si content dependence of P_{O_2} for EY, EY/E*n* and EY/EE′. Content of EY component in copolymer is 50 mol%

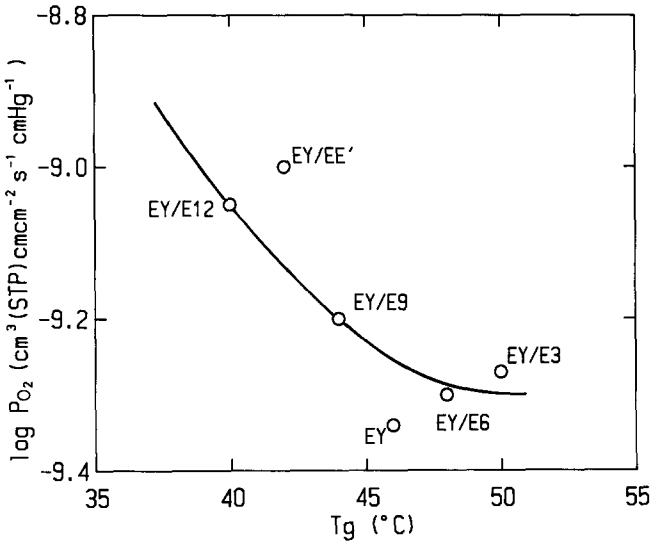

Figure 12 Plots of P_{O_2} against T_g for EY, EY/E*n* and EY/EE′. Content of EY component in copolymer is 50 mol%

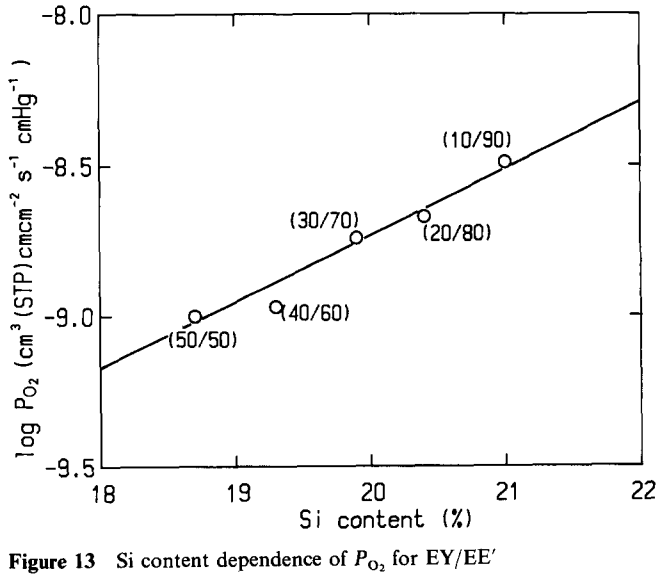

Figure 13 Si content dependence of P_{O_2} for EY/EE′

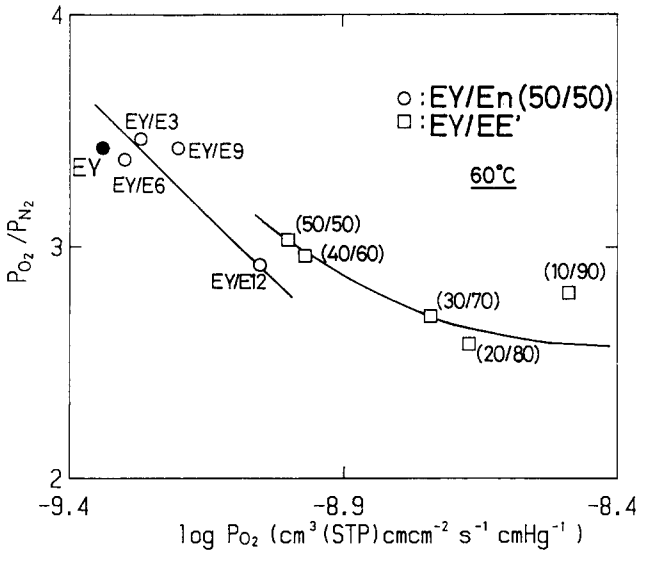

Figure 14 Plots of P_{O_2}/P_{N_2} against P_{O_2} for all network films studied

that for EY/E*n*. In other words, EY/EE' has higher P_{O_2}/P_{N_2} compared with the extrapolated value from EY/E*n*. This result implies that the increase of EE' component, the increase of siloxane moiety, causes a higher oxygen permeability with a smaller decrease of separation factor.

CONCLUSIONS

Oxygen and nitrogen permeabilities of silicon-containing network polymer films of EY, EY/E*n* and EY/EE' have been investigated.

These network polymer films were prepared through soluble prepolymers and subsequent post-polymerization of cast prepolymer films. Post-polymerized films were flexible, transparent and insoluble in common solvents.

Oxygen and nitrogen permeabilities increased with increasing temperature. EY homopolymer had P_{O_2} of 4.6×10^{-10} cm^3(s.t.p.) cm cm^{-2} s^{-1} $cmHg^{-1}$ and P_{O_2}/P_{N_2} of 3.4 at 60°C. The slope of the Arrhenius plot of permeability coefficient changed at a certain temperature T_i, which corresponds well to T_g of these network polymers. Incorporation of copolymer component of E*n* and EE' enhanced the oxygen and nitrogen permeabilities with decreasing T_g. The decrease of T_g increased P_{O_2}, which may be explained by enhancement of the flexibility of the molecular chain. For EY/EE', increase of E' component gave rise to an increase of P_{O_2} with a smaller decrease of P_{O_2}/P_{N_2}. EY/EE'(10/90 mol%) film had the highest value of P_{O_2} of 3.2×10^{-9} cm^3(s.t.p.) cm cm^{-2} s^{-1} $cmHg^{-1}$ and P_{O_2}/P_{N_2} of 2.8 at 60°C. It is noted that the introduction of network structure by copolymerization of Y with EE' polymer enables a film to be formed, although EE' homopolymer has less processability to make a film.

ACKNOWLEDGEMENTS

The authors are sincerely grateful to Chisso Corporation for providing the siloxane-containing monomers and to Sanyo Chemical Industries for the gas permeation facility. They also thank Dr K. Matsumoto, Kyoto Institute of Technology, and Professor M. Nagata, Junior Women's College, Kyoto Prefectural University, for their useful comments.

REFERENCES

1 Speck, S. B. *J. Org. Chem.* 1953, **18**, 1689
2 Kovacs, H. N., Delman, A. D. and Simms, B. B. *J. Polym. Sci. (A-1)* 1968, **6**, 2103
3 Kovacs, H. N., Delman, A. D. and Simms, B. B. *J. Polym. Sci. (A-1)* 1968, **6**, 2117
4 Pratt, J. R. and Johnston, N. J. *Polym. Eng. Sci.* 1976, **16**, 309
5 Kondo, H., Sato, M. and Yokoyama, M. *Eur. Polym. J.* 1982, **18**, 181
6 Kondo, H., Sato, M. and Yokoyama, M. *J. Polym. Sci., Polym. Chem. Edn.* 1983, **21**, 21
7 Ghatge, N. D. and Jadhav, J. Y. *J. Polym. Sci., Polym. Chem. Edn.* 1984, **22**, 1565
8 Nakagawa, T. *Chem. Chem. Ind.* 1982, **35**, 842
9 Kiyotsukuri, T., Tsutsumi, N., Ayama, K. and Nagata, M. *J. Polym. Sci. (A) Polym. Chem.* 1987, **25**, 1591
10 Kiyotsukuri, T., Tsutsumi, N., Ayama, K. and Nagata, M. *J. Polym. Sci. (A) Polym. Chem.* 1988, **26**, 807
11 Tsutsumi, N., Tsuji, A., Horie, C. and Kiyotsukuri, T. *Eur. Polym. J.* 1988, **24**, 837
12 Tsutsumi, N., Mimaki, M., Nagura, K. and Kiyotsukuri, T. *Polym. Commun.* 1990, **31**, 132
13 Kiyotsukuri, T., Tsutsumi, N. and Chen. Y. *Polym. Commun.* 1990, **31**, 17
14 Kiyotsukuri, T., Tsutsumi, N. and Chen, Y. *J. Polym. Sci. (A) Polym. Chem.* 1990, **28**, 1197
15 Tsutsumi, N., Chen, Y. and Kiyotsukuri, T. *J. Polym. Sci. (A) Polym. Chem.* in press
16 Kiyotsukuri, T., Tsutsumi, N., Sugimoto, M. and Saito, N. *Polym. Commun.* 1990, **31**, 56